

Lawrence Berkeley National Laboratory

Recent Work

Title

ASYMPTOTIC PLANARITY: AH S-MATRIX BASIS FOR THE OKUBO-ZWEIG-IIZUKA RULE

Permalink

<https://escholarship.org/uc/item/7pk9706c>

Author

Chew, G.F.

Publication Date

1975-10-01

Submitted to Nuclear Physics B

RECEIVED
LIBRARY
NOV 21 1975
LIBRARY
DOCUMENTS SECTION

LBL-4603
Preprint

c.1

ASYMPTOTIC PLANARITY: AN S-MATRIX BASIS FOR
THE OKUBO-ZWEIG-IZUKA RULE

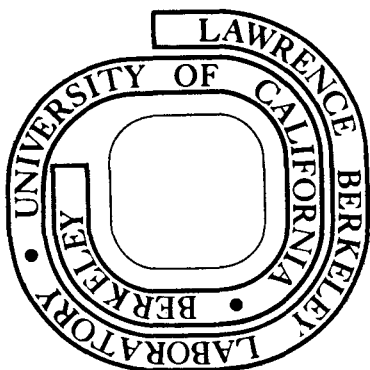
G. F. Chew and C. Rosenzweig

October 7, 1975

For Reference

Not to be taken from this room

Prepared for the U. S. Energy Research and
Development Administration under Contract W-7405-ENG-48



1
2
3
4
5
6
7
8
9
0
1
2
3
4
5
6
7
8
9
0

DISCLAIMER

This document was prepared as an account of work sponsored by the United States Government. While this document is believed to contain correct information, neither the United States Government nor any agency thereof, nor the Regents of the University of California, nor any of their employees, makes any warranty, express or implied, or assumes any legal responsibility for the accuracy, completeness, or usefulness of any information, apparatus, product, or process disclosed, or represents that its use would not infringe privately owned rights. Reference herein to any specific commercial product, process, or service by its trade name, trademark, manufacturer, or otherwise, does not necessarily constitute or imply its endorsement, recommendation, or favoring by the United States Government or any agency thereof, or the Regents of the University of California. The views and opinions of authors expressed herein do not necessarily state or reflect those of the United States Government or any agency thereof or the Regents of the University of California.

ASYMPTOTIC PLANARITY:

AN S-MATRIX BASIS FOR THE OKUBO-ZWEIG-IIZUKA RULE*

G. F. Chew and C. Rosenzweig[†]Department of Physics and Lawrence Berkeley Laboratory
University of California, Berkeley, California 94720

October 7, 1975

ABSTRACT

A mechanism is exhibited that monotonically depresses the cylinder component of the topological expansion with increasing t , and it is conjectured that all nonplanar S-matrix components diminish as t increases, exchange degeneracy and the Okubo-Zweig-Iizuka rule becoming more accurately satisfied. Such asymptotic planarity is compared to the field-theoretical concept of asymptotic freedom. The characteristic low- t cylinder "quenching interval" is found to be the inverse of the mean value over a two-reggeon loop, of $\frac{1}{2} \pi^2 (\alpha')^2 (t_1 - t_2)^2 / (-t)$, where t_1 and t_2 are the squared masses of the loop reggeons and α' is the trajectory slope. For leading trajectories the low- t cylinder quenching interval is predicted by this formula to be roughly 0.5 GeV^2 --consistent with the observed pomeron intercept and slope, with the ρ - ω and f - A_2 mass differences and with the (ϕ, ω) deviation from ideal mixing. As t grows negatively over a corresponding interval, it is predicted that the pomeron will become nearly a pure SU_3 singlet. If the pion mass helps to set the scale for reggeon loops coupled to unnatural-parity trajectories, the cylinder quenching interval will be larger--explaining the large (η, η')

deviation from ideal mixing as well as the large π - η mass difference. Even when the small- t cylinder quenching is rapid ("precocious planarity") the large- t approach to the planar limit turns out to be gentle. A by-product of this study is an explanation of the approximate reality and linearity of trajectories at large t .

I. INTRODUCTION

Two sets of striking experimental facts, the exchange degeneracy of high-lying Regge trajectories and the validity of the Okubo-Zweig-Iizuka (OZI) ideal-mixing selection rules for particles on these trajectories, can be combined into the statement that the hadron S matrix in certain regions is approximately planar. The adjective "planar" describes the leading component of Veneziano's topological expansion¹--a component characterized by the combination of exchange degeneracy with ideal mixing. Substantial nonplanar (e.g., pomeron) effects are experimentally observed near $t = 0$, but along leading trajectories these have largely disappeared already at the first physical vector mesons (ρ , ω , ϕ), which exhibit a high degree of exchange degeneracy and ideal mixing. In the Ψ -particle region, the tiny widths of the new particles suggest that nonplanar effects have become still smaller. Such a growing accuracy of the planar approximation as mass increases has been called "asymptotic planarity".²

Because key properties of the planar approximation are shared by simple quark models, the physical content of asymptotic planarity--an S-matrix concept--is related to that of asymptotic freedom--a field-theoretic concept--but the former has been studied far less than

[†] Present address: Physics Department, University of Pittsburgh, Pittsburgh, PA 15260.

00004408238

the latter. The objective of this paper is to extend understanding of both the theoretical origin and the experimental meaning of asymptotic planarity.

Leading corrections to the planar S matrix correspond to nonplanar diagrams such as shown in Fig. 1--corrections extensively studied in Refs. (2 - 4). For $t \leq 0$, Fig. 1a--called by Veneziano a "cylinder" correction--has long been associated with pomeron exchange. In Ref. (2) it was shown that, more generally, this cylinder correction shifts all isosinglet planar trajectories and alters their couplings away from ideal mixing. The f trajectory, in particular, is shifted upward near $t = 0$ and becomes closer to an SU_3 singlet; the shifted f is the pomeron. Other isosinglet trajectories, such as f' , ω and ϕ , are also shifted and the corresponding coupling shifts of physical particles on these trajectories correspond to violations of the OZI rule. Pomeron prominence and OZI-rule violations are thus, both, manifestations of the cylinder shift, the difference being only in the value of t . This paper studies continuation of the cylinder shift from $t \leq 0$ to positive values of t where particle poles appear.

It was observed in Ref. (2) that according to experiment, the f trajectory possesses a prominent SU_3 -singlet component at $t = 0$ while at the same time behaving like a nearly ideally-mixed system at $t = m_f^2$. The spacing between f (pomeron) and A_2 near $t = 0$ is correspondingly much wider than near $t = m_f^2$. Analogous statements may be made about the entire leading isosinglet family (f, ω, f', ϕ). In the present paper we exhibit a theoretical mechanism to explain the foregoing. Our mechanism stems from planar Regge behavior and

suppresses the cylinder as t grows in the positive direction. The mechanism works in the reverse sense for negative t --enhancing the cylinder--and since no experimental indication exists for planarity at large negative t we are led to propose a one-sided status for "planar asymptopia". It is in fact plausible that the cylinder may become a dominant effect at negative t , the pomeron becoming more and more nearly a pure SU_3 singlet. We shall show that our positive- t cylinder-quenching mechanism is capable of correlating the prominent nonplanar effects observed for $t \leq 0$ with the smallness of such effects for $t \geq 0.5 \text{ GeV}^2$ along the leading vector-tensor trajectories.

We find that, following a sharp initial decrease of cylinder strength (precocious planarity), the asymptotic approach to pure planar couplings is gentle--a circumstance reminiscent of that encountered in asymptotically free field theories. The rate of initial decrease in our mechanism is determined by the masses of low-lying physical mesons, such as the ρ . The cylinder "quenching interval" in t varies inversely with these masses, so when the π mass is important, as seems likely for unnatural parity trajectories, cylinder suppression is initially less rapid. Our mechanism thus promises to explain the relatively large degree of nonplanarity experimentally exhibited in the (η, η') system.

The mechanism leads to a monotonic decrease (without sign change) in the real part of the cylinder correction to the leading natural parity trajectories. When combined with the charge-conjugation considerations developed in Ref. (2), such behavior correctly predicts that $m_f^2 < m_{A_2}^2$ while $m_\rho^2 < m_\omega^2$. A corresponding statement is that cylinder rotations away from ideal mixing are in opposite (but predictable) directions for tensor and vector mesons.

We proceed now in the following three sections to derive the foregoing results.

II. A CYLINDER-QUENCHING MECHANISM FOR POSITIVE t

In the analysis of Ref. (2) attention was directed to a cylinder twist operator $C(t)$ whose matrix elements acting in the space of planar Regge poles could be depicted as in Fig. 2, the index i labeling the sequence of planar poles. Cylinder corrections to the planar S matrix are determined by this operator. The question at issue is why $C(t)$ should be much smaller for $t \gtrsim 1 \text{ GeV}^2$ than for $t \leq 0$.

Let us suppose that the loop in Fig. 2 can be represented by a helicity-pole expansion as in Fig. 3. The well-known two dimensional region of integration over dt_1 and dt_2 will be treated below in detail. The integrand contains two triple-Regge vertices together with Regge "propagators" for the dashed links. The fact that each link is twisted means that the Regge phase factor $e^{i\pi\alpha_j}$, which would be carried by a corresponding planar link, is to be replaced by 1. For the loop as a whole the factor $\cos \pi(\alpha_{j_1}(t_1) - \alpha_{j_2}(t_2))$ constitutes the only distinction between twisted and planar loops; our task is to understand why, as t grows in the positive direction, such a seemingly minor difference can make twisted loops much smaller than the corresponding planar loops.

The mechanism is easy to exhibit for small positive t --below the first normal threshold associated with the loop in question. In this region the loop phase space may conveniently be expressed through variables k and w such that⁵

$$t_{1,2} = \frac{1}{4}t - k^2 - w^2 \pm w(-t)^{\frac{1}{2}}. \quad (\text{II.1})$$

One finds

$$\int d\phi_{12} \rightarrow \int_0^\infty dk \int_{-\infty}^\infty dw, \quad (\text{II.2})$$

the limits of integration being independent of t . When t passes the point $t_0 = 4m^2$, m being the mass of the first physical particle on a loop trajectory, the integral over dw must be appropriately deformed, but below this threshold the integration variables k and w are everywhere real. In consequence the difference $t_1 - t_2$ is pure imaginary for $0 < t < t_0$:

$$t_1 - t_2 = 2iw(t)^{\frac{1}{2}}. \quad (\text{II.3})$$

If the loop trajectories are approximately linear functions of t_1 and t_2 with the same slope, then

$$\alpha_{j_1}(t_1) - \alpha_{j_2}(t_2) \approx \alpha_{j_1}(0) - \alpha_{j_2}(0) + \alpha'(t_1 - t_2) \quad (\text{II.4})$$

and the factor which for negative t was oscillatory develops exponential behavior in $(t)^{\frac{1}{2}}$. For example, if α_{j_1} and α_{j_2} are the same trajectory, α_j ,

$$\cos \pi(\alpha_j(t_1) - \alpha_j(t_2)) \rightarrow \cosh 2\pi\alpha'w(t)^{\frac{1}{2}} \quad (\text{II.5})$$

so the untwisted loop becomes larger than the twisted loop, the effect growing with t . Although the magnitude of the difference between twisted and untwisted loops depends on other factors in the loop integral that determine the relative contributions from different intervals in w , one may characterize the factor suppressing the twisted loop (enhancing the untwisted loop) as the mean value

00004408239

$$\langle \cosh 2\pi \alpha' w (t)^{\frac{1}{2}} \rangle. \quad (\text{II.6})$$

Consistency with the planar bootstrap requirement^{6,7} means that the vertex factors in the planar loop must compensate this strong increase from the Regge phase factor, giving the planar loop an essentially constant strength for all values of t . (See Eq. (III.1) below.) In the twisted loop it is these same vertex factors--unbalanced by (II.6)--that produce a strong decrease in the cylinder operator $C(t)$. We do not, however, require a detailed understanding of the vertex factors to estimate the ratio between twisted and untwisted loops.

Near $t = 0$ we may expand (II.6) to define a characteristic "cylinder quenching" interval. That is, since

$$\cosh 2\pi \alpha' w (t)^{\frac{1}{2}} \approx 1 + 2\pi^2 \alpha'^2 w^2 t \quad (\text{II.7})$$

the cylinder is substantially extinguished within the interval

$$t_c = \frac{1}{2\pi^2 \alpha'^2 \langle w^2 \rangle_{t=0}}. \quad (\text{II.8})$$

In the following section we estimate $\langle w^2 \rangle_{t=0}$ in a simple example.

III. AN ESTIMATE OF THE SMALL- t CYLINDER-QUENCHING INTERVAL

Let us consider a diagonal element of $C(t)$ with respect to a leading planar Regge pole (f, ω, ρ, A_2) , with this same trajectory appearing in both links of the loop. Figure 2 then simplifies to Fig.4. The corresponding untwisted loop has been studied by Veneziano and collaborators⁶⁻⁸ in connection with a planar bootstrap model, and we shall borrow from their observations about triple-Regge vertices and

reggeon propagators.

A typical bootstrap equation for the planar loop is^{6,7}

$$1 = \Gamma(\alpha(t)) \int d\theta_{12} G^2(t, t_1, t_2) \Gamma(1 - \alpha(t_1)) \Gamma(1 - \alpha(t_2)) \\ \times \cos \pi(\alpha(t_1) - \alpha(t_2)); \quad (\text{III.1})$$

where we shall refer to the Γ functions inside the integrand as "propagators". The vertex factor $G(t, t_1, t_2)$ is expected to produce a strong cutoff at large values of the quantity $\alpha(t) - \alpha_c(t_1, t_2)$, where

$$\alpha_c(t_1, t_2) = \alpha(t_1) + \alpha(t_2) - 1. \quad (\text{III.2})$$

Since

$$\alpha - \alpha_c \approx 1 - \alpha(0) + 2\alpha' \left(\frac{1}{4} t + k^2 + w^2 \right), \quad (\text{III.3})$$

such a cutoff not only ensures convergence of the loop integral but guarantees that $\langle k^2 + w^2 \rangle \lesssim 1/\alpha'$. Obviously $\langle w^2 \rangle \lesssim 1/\alpha'$, but we would like a sharper estimate.

Using simple multiperipheral and dual-resonance models as a guide, following Ref. (6,7), it appears that for k^2, w^2 and t all small the variation of the loop integrand will be dominated by the first physical-particle poles in the loop propagators $\Gamma(1 - \alpha_{1,2})$ together with the "threshold" behavior of the vertices. Since the squared magnitude of the loop momentum is

$$\frac{1}{4t} \lambda(t, t_1, t_2) = k^2, \quad (\text{III.4})$$

while the "orbital" angular momentum of the loop is $\alpha - \alpha_c - 1$, one

expects a "centrifugal barrier" suppression factor^{*} proportional to $k^{2(\alpha-\alpha_c)}$, effective for $k^2 \lesssim m^2$, where m is the smallest relevant particle mass--controlling the "range of the force". In our example, this is the ρ mass. At the same time the ρ poles in the propagator product $\Gamma(1-\alpha_1)\Gamma(1-\alpha_2)$ give a dependence

$$\frac{1}{(t_1 - m_\rho^2)(t_2 - m_\rho^2)} \Big|_{t=0} = \frac{1}{(k^2 + w^2 + m_\rho^2)^2}, \quad (\text{III.5})$$

so the scale on both counts is set by m_ρ^2 --a fact whose importance we shall see later. Because the combination $k^2 + w^2$ appears in (III.5), it is convenient to change variables from (k, w) to (u, θ) , where

$$\begin{aligned} u &= k^2 + w^2 \\ \theta &= \tan^{-1} k/w, \end{aligned} \quad (\text{III.6})$$

with

$$\int d\phi_{12} \rightarrow \int_0^\infty du \int_0^\pi d\theta \quad (\text{III.7})$$

and ask for the average value

$$\langle w^2 \rangle = \langle u \cos^2 \theta \rangle \quad (\text{III.8})$$

$$\approx \langle u \rangle \langle \cos^2 \theta \rangle. \quad (\text{III.9})$$

* From the s-channel viewpoint, such a factor represents the kinematical lower limit constraint on $t_{1,2}$. The mass m is then the minimum mass of an important cluster in the multiperipheral chain.

What is a reasonable estimate for $\langle \cos^2 \theta \rangle$? If the chief dependence on θ arises from the threshold factor

$$(k^2)^{\alpha-\alpha_c} = u^{\alpha-\alpha_c} (\sin^2 \theta)^{\alpha-\alpha_c}, \quad (\text{III.10})$$

we easily calculate

$$\langle \cos^2 \theta \rangle \approx \frac{1}{2(1 + \alpha - \alpha_c)}, \quad (\text{III.11})$$

or, in view of (III.3) rewritten as

$$\alpha - \alpha_c \Big|_{t=0} \approx \alpha' \left[m_\rho^2 + 2u \right], \quad (\text{III.12})$$

we have

$$\langle \cos^2 \theta \rangle \approx \frac{1}{2 \left[1 + \alpha' (m_\rho^2 + 2\langle u \rangle) \right]}. \quad (\text{III.13})$$

Our result, then, is

$$\langle w^2 \rangle \approx \frac{\langle u \rangle}{2 \left[1 + \alpha' (m_\rho^2 + 2\langle u \rangle) \right]}. \quad (\text{III.14})$$

so with

$$\langle u \rangle \sim m_\rho^2 \approx 1/2\alpha', \quad (\text{III.15})$$

an estimate that we have verified by a more careful numerical calculation, we find

$$\langle w^2 \rangle \approx \frac{1}{5} m_\rho^2. \quad (\text{III.16})$$

corresponding to

$$t_c \approx \frac{5}{2\pi^2 (\alpha')^2 m_\rho^2} \approx 0.5 \text{ GeV}^2. \quad (\text{III.17})$$

The cylinder is thus substantially quenched by the time one reaches the lowest-lying physical vector mesons.

Assuming all leading trajectories to have similar slopes, we have found that the small- t cylinder quenching interval depends inversely on the mass of the lowest-lying physical particle occurring in the reggeon loop or within the chain of singularities that build the pole under study. Formula (II.8) expresses t_c through the reciprocal of $\langle w^2 \rangle_{t=0}$ and this mean value, quite naturally, reflects the lowest relevant particle masses.

A consequence of the foregoing is that if m_ρ^2 were smaller than $1/2\alpha'$, the leading vector mesons would be less planar. Why is the π mass not important for the vector-tensor trajectories when one considers loops such as shown in Fig. 5? This is an old question, and the answer here is the same as in countless models that have attempted to represent ρ and f as $\pi\pi$ composites. The loop orbital angular momentum, even near $t = 0$, is sufficiently high that the threshold (centrifugal repulsion) factor suppresses the pion poles in the reggeon propagators. The contribution of the pion loop, relative to the vector-tensor loop of Fig. 4, is thereby reduced, as is the importance of the physical pion pole in determining $\langle w^2 \rangle$. It is the ρ mass--controlling the "range of the force" between two pions--that tends to set the scale of the pion loop so, even if the pion loop is significant, the rate of cylinder damping remains as estimated above.

On the other hand, what about a loop such as in Fig. 6, which we would expect to be important for the properties of unnatural-parity Regge poles. Here the orbital angular momentum is similar to that of Fig. 4 (lower than in Fig. 5) so the pion propagator pole will be more prominent. Furthermore the "range of the force" between π and f will reflect the π mass. A careful calculation is needed to establish the scale of cylinder damping in this case, but experience with the somewhat analogous pion-nucleon loop suggests that when the two lowest loop masses are different the scale is set by their geometric mean. We might then guess the scale t_c of cylinder suppression for an unsymmetrical loop like that of Fig. 6 to be a factor $m_\rho/m_\pi \approx 5$ longer than that for the symmetrical loop considered in Sec. III. The cylinder would consequently not be quenched until $t \gtrsim 2 \text{ GeV}^2$.

Note that there are two reasons for low-mass mesons of unnatural parity to exhibit less exchange degeneracy and a higher degree of OZI-rule violation than natural-parity mesons. Even if the cylinder-quenching interval were the same as for natural parity, the lower mass of (π, η) in comparison to (ρ, ω) would make the former particles less planar. The larger quenching interval further enhances the difference.

Masses larger than m_ρ may be expected to control the cylinder quenching interval for trajectories associated with higher-threshold conserved quantum numbers. If charm exists, for example, the scale of cylinder quenching for a charmonium trajectory would be set (inversely) by the mass of the lowest-lying charmed meson. This mass is expected to be substantially greater than m_ρ , so asymptopia should be even more precocious than along the leading trajectories.

IV. CONTINUATION BEYOND THE FIRST THRESHOLD IN t

If we wish to calculate the mean value (II.6) at values of t near or above the first threshold, a complication arises from the leading particle poles in the reggeon propagators. For a fixed real value of k , the poles at $t_{1,2} = m_{1,2}^2$ occur at

$$w = i \left[\pm (k^2 + m_1^2)^{\frac{1}{2}} + \frac{1}{2} t^{\frac{1}{2}} \right] \quad (\text{IV.1})$$

and

$$w = i \left[\pm (k^2 + m_2^2)^{\frac{1}{2}} - \frac{1}{2} t^{\frac{1}{2}} \right]. \quad (\text{IV.2})$$

For small t these poles reside on the imaginary w axis, away from the contour of integration, but one of each pair heads towards the real axis as t increases, crossing the axis at $t = 4(k^2 + m_{1,2}^2)$. The w contour may be deformed to allow a continuation in t but there will ultimately be a contour-pinching collision between the upward-moving m_1 -associated pole, that starts below the real axis, and the downward-moving m_2 -associated pole, that starts above the real axis. This collision occurs at

$$t^{\frac{1}{2}} = (k^2 + m_1^2)^{\frac{1}{2}} + (k^2 + m_2^2)^{\frac{1}{2}}, \quad (\text{IV.3})$$

the point where energy is conserved for physical particles of masses m_1 and m_2 . To continue past this point we must exercise care.

After both poles have crossed the real axis, the original w contour will have been deformed as shown in Fig. 7a, which is equivalent to the sum of the three contours in Fig. 7b. In other words, for $t > \left((k^2 + m_1^2)^{\frac{1}{2}} + (k^2 + m_2^2)^{\frac{1}{2}} \right)^2$ we must supplement the integral along the real w axis by the sum of two residues. As

t increases further more poles will cross the real axis and more residue terms correspondingly will augment the real-axis integral. We do not propose here to calculate the added terms but direct attention to an important qualitative feature thereof: Each pole residue is evaluated at an integer value of α_1 with α_2 a real function of k and t , or vice-versa (w is pure imaginary). The factor $\cos \pi(\alpha_1 - \alpha_2)$ is thus an oscillating function and does not grow in magnitude. Growth occurs only in the integral along the real axis.

Since imaginary parts of loop integrals arise entirely from pole residues, the effect to which we are here drawing attention tends to make Regge trajectories predominantly real (and therefore linear). A related remark is that resonance partial widths get comparable contributions from twisted and untwisted loops. It is only in its real part that the positive- t untwisted loop is larger than the twisted.

The pole-residue contributions to the w integral have both real and imaginary parts and one expects the former to be of the same order of magnitude as the latter, especially for twisted loops where the oscillating factor $\cos \pi(\alpha_1 - \alpha_2)$ is missing. In what follows we concentrate attention on the contribution to $\text{Re } C(t)$ from the integral along the real w axis, ignoring the pole contributions to $\text{Re } C(t)$ on the grounds that they are of the same order as $\text{Im } C(t)$. To the extent that the leading trajectories tend to be linear--with small imaginary parts--such an approach is justified.

How large a ratio of untwisted to twisted real parts do we expect for large t ? Let us return to our simple example in order to achieve an estimate.

0.0004408241

V. LARGE-t CYLINDER QUENCHING

The present state of ignorance about the large-t behavior of triple-Regge vertex functions rules out confident estimates of cylinder quenching for $t \gg m_\rho^2$. We nevertheless here draw attention to a mechanism that tends to smooth out the initially exponential form of cylinder damping. This mechanism stems from the reggeon propagators which, as we shall show, favor mean values of $\langle w^2 \rangle$ that diminish with increasing t .

A plausible form for the propagator product in Fig. 4 is $\Gamma(1 - \alpha_1)\Gamma(1 - \alpha_2)$, and for the integral along the real axis, away from the poles on the imaginary axis, it should be legitimate to use the Stirling formula

$$\Gamma(z) \propto \left(\frac{z}{e}\right)^{z-\frac{1}{2}} \quad (V.1)$$

Since

$$1 - \alpha_{1,2} = k^2 + w^2 + m_\rho^2 - \frac{1}{4}t \pm iw(t)^{\frac{1}{2}}, \quad (V.2)$$

using units where $\alpha' = 1$, we have

$$\Gamma(1 - \alpha_1)\Gamma(1 - \alpha_2) \propto \left(\frac{\Delta^2 + w^2 t}{e^2}\right)^{\Delta-\frac{1}{2}} \exp\left[-2w(t)^{\frac{1}{2}} \tan^{-1} \frac{w(t)^{\frac{1}{2}}}{\Delta}\right], \quad (V.3)$$

where

$$\Delta \equiv k^2 + w^2 + m_\rho^2 - t/4. \quad (V.4)$$

The branch of the arctangent in the exponent of (V.3) is such that

$$\begin{aligned} \tan^{-1}(w(t)^{\frac{1}{2}}/\Delta) &\sim w(t)^{\frac{1}{2}}/\Delta \\ w(t)^{\frac{1}{2}} &\rightarrow 0 \\ \Delta &> 0 \end{aligned} \quad (V.5)$$

while

$$\begin{aligned} \tan^{-1}(w(t)^{\frac{1}{2}}/\Delta) &\rightarrow \pm \pi \\ w(t)^{\frac{1}{2}} &\rightarrow \pm 0 \\ \Delta &< 0 \end{aligned} \quad (V.6)$$

Because the exponent $-2w(t)^{\frac{1}{2}} \tan^{-1}(w(t)^{\frac{1}{2}}/\Delta)$ is always negative, the propagator factor (V.3) tends to favor small values of $w(t)^{\frac{1}{2}}$. In particular, for $t \gg 4(k^2 + w^2 + m_\rho^2)$, where Δ is large and negative, this exponent approaches $-2\pi w(t)^{\frac{1}{2}}$, exactly the same argument appearing in the cylinder-suppression factor, $\cosh 2\pi w(t)^{\frac{1}{2}}$. This is no accident since, for α_1 and α_2 equal to integers the original factor $\cos \pi(\alpha_1 - \alpha_2)$ is equal to $(-1)^{\alpha_1 - \alpha_2}$, giving the sign alternation precisely required to compensate the alternating sign of the pole residues in the Γ functions--so that the net sign of every planar pole residue is positive. Now, even though the Stirling formula contains no poles, it must reflect the alternating sign of the poles in $\Gamma(1 - \alpha_1)\Gamma(1 - \alpha_2)$ so one should not be surprised to find Formula (V.3) tending to compensate the analytic continuation of $\cos \pi(\alpha_1 - \alpha_2)$. In any event, the reggeon propagators favor w values of the order $1/(t)^{\frac{1}{2}}$ in the integral along the real w axis.

To proceed further we assume that the vertex functions give separate (multiplicative) cutoffs in k^2 and w^2 and consider values of t such that

$$\frac{1}{4}t \gg k_{\max}^2 + w_{\max}^2 + m_\rho^2. \quad (V.7)$$

The last factor in (V.3) then leads to the estimate

$$\langle \cosh 2\pi w(t)^{\frac{1}{2}} \rangle \approx \frac{\int_0^{w_{\max}} dw \cosh[2\pi w(t)^{\frac{1}{2}}] \exp[-2\pi w(t)^{\frac{1}{2}}]}{\int_0^{w_{\max}} dw \exp[-2\pi w(t)^{\frac{1}{2}}]} \quad (V.8)$$

$$\approx \frac{\frac{1}{2} w_{\max}}{(2\pi (t)^{\frac{1}{2}})^{-1}} = \pi (t)^{\frac{1}{2}} w_{\max} \quad (V.9)$$

The rate of cylinder quenching has been slowed to an inverse square root.

To contrast the low- t and high- t estimates of cylinder quenching let us set $w_{\max} \approx m_{\rho}$. The results of this section and that of Sec. III are then combined in Fig. 8. We do not take too seriously our high- t estimate but believe the qualitative feature that cylinder damping slows from the precipitous initial rate.

VI. APPLICATIONS TO EXPERIMENT

A. Pomeron Properties for $t \leq 0$

One manifestation of the cylinder quenching interval t_c is the difference between the slopes of pomeron and rho trajectories near $t = 0$. According to Ref. (2) the displacement of the pomeron (f) above the ρ arises from twisted loops of the form of Fig. 4. That is, if

$$\alpha_p(t) = \alpha_{\rho}(t) + \Delta\alpha(t), \quad (VI.1)$$

the shift $\Delta\alpha(t)$ is approximately given by a superposition of such loops. We have defined the parameter t_c so that the logarithmic derivative of a twisted loop differs at $t = 0$ from that of the corresponding untwisted loop by $-1/t_c$. The corresponding statement for the difference between pomeron and rho trajectories is

$$\left[\frac{(\Delta\alpha)'}{\Delta\alpha} \right]_{t=0} \approx -\frac{1}{t_c}, \quad (VI.2)$$

or

$$t_c \approx \frac{\alpha_p(0) - \alpha_{\rho}(0)}{\alpha'_{\rho}(0) - \alpha'_p(0)}. \quad (VI.3)$$

Such a formula corresponds to the statement that at $t = t_c$, where the cylinder correction has become nearly quenched, the displacement between pomeron and rho will have become much smaller than at $t = 0$. This requirement, as seen in Fig. 9, immediately implies a pomeron slope less than the rho slope. The lowering of the pomeron slope through action of the factor $\cos \pi(\alpha_1 - \alpha_2)$ was discovered by Chan, Paton and Tsou.⁹

The observed $t = 0$ intercept difference between pomeron and rho is about 0.4, while the slope difference appears to be in the neighborhood of 0.6 GeV^{-2} . The estimate made above in Sec. III, $t_c \approx 0.5 \text{ GeV}^2$, is thus in satisfactory accord with (VI.3). It is noteworthy that according to (VI.3), if the pomeron slope at $t = 0$ is not to become negative, the cylinder quenching interval may not be smaller than $[\alpha_p(0) - \alpha_{\rho}(0)]/\alpha'_{\rho}(0)$.

Because the cylinder operator $C(t)$ is analytic near $t = 0$ it is to be expected that the cylinder is much larger for $t \lesssim -t_c$ than for $t = 0$, making the pomeron more nearly an SU_3 singlet. Higher terms in the topological expansion, corresponding to pomeron-pomeron cuts, will probably then also be important, but one may look qualitatively for high-energy diffraction to be closer to SU_3 singlet in character for $t \lesssim -t_c$ than for $t = 0$. A comparison of experimental differential elastic πp with Kp and of ρp with ϕp cross sections should show a trend toward equality as t becomes more negative.

An associated qualitative expectation is that for $t < -t_c$ the pomeron trajectory will be pushed as far above the rho trajectory as allowed by general principles; i.e., one looks for the pomeron at large negative t to be relatively flat, the slope becoming even smaller than at $t = 0$.

B. Violation of Exchange Degeneracy and OZI-Rule for Vector and Tensor Mesons

In Ref. (2) a model was formulated for the cylinder shift of the six leading trajectories carrying zero quantum numbers: f , ρ^0 , A_2^0 , ω , f' , ϕ . The assumption of SU_3 symmetry allowed the model to be characterized by a single function $k(t)$, measuring the cylinder coupling between planar trajectories; the mechanism of the present paper may correspondingly be condensed into the rough statement

$$\text{Re } k(t) \approx \frac{k(0)}{\langle \cosh 2\pi w(t)^{\frac{1}{2}} \rangle} \quad (\text{VI.4})$$

As discussed above in Sec. IV the imaginary part of $k(t)$ arises from

poles at imaginary values of w and cannot be estimated by such a formula. Additionally, because the imaginary part is closely associated with physical thresholds, the assumption of SU_3 symmetry is unreasonable. (For $t < 1 \text{ GeV}^2$, for example, the imaginary parts of f and ρ trajectories arise almost entirely from the $\pi\pi$ channel, with no contribution from $K\bar{K}$.) Our comparison with experiment will therefore be limited to the real part of the cylinder coupling, assuming this to arise in an approximately SU_3 -symmetrical fashion primarily from the integral along the real w axis.

It was shown in Ref. (2) that

$$k(0) = 0.15 \pm 0.05 \quad (\text{VI.5})$$

and for $t \gtrsim t_c$ we expect $k(t)$ to have become so small that first-order perturbation theory is ample. The first-order trajectory shifts, according to Formulas (VII.3') and (VII.4) of Ref. (2), are given by

$$\text{Re}(\alpha_f(t) - \alpha_{A_2}(t)) \approx \text{Re}(\alpha_\rho(t) - \alpha_\omega(t)) \approx 2 \text{Re } k(t). \quad (\text{VI.6})$$

Since

$$\text{Re}(\alpha_f - \alpha_{A_2})_{t=m_{A_2}^2} \approx \alpha' \text{Re}(m_{A_2}^2 - m_f^2) \quad (\text{VI.7})$$

$$\text{Re}(\alpha_\rho - \alpha_\omega)_{t=m_\rho^2} \approx \alpha' \text{Re}(m_\omega^2 - m_\rho^2) \quad (\text{VI.7}')$$

we may employ (VI.6) to obtain values for $k(t)$ at $t = m_\rho^2$ and $t = m_{A_2}^2$ insofar as the real parts of the (A_2 , f , ρ , ω) masses (pole positions) are known. The signs of these real part differences,

as given by experimental Breit-Wigner parameters, are as predicted from (VI.4), but non-negligible imaginary parts prevent determination of more than the order of magnitude of $k(t)$. (Experience with the Δ resonance shows that when a resonance width is $\gtrsim 100$ MeV the real part of the mass may be shifted by as much as 20 MeV from the Breit-Wigner value.) One can infer only that

$$\text{Re } k(t = m_\rho^2) \lesssim 0.03, \quad \text{Re } k(t = m_{A_2}^2) \lesssim 0.04. \quad (\text{VI.8})$$

Such numbers are in comfortable accord with $k(0) = 0.15 \pm 0.05$ together with our estimate $t_c \sim 0.5 \text{ GeV}^2$.

A more precise determination of $k(t)$ in the intermediate- t region emerges from the observed OZI-rule violation of vector mesons--their deviation from ideal mixing. A standard measure of this violation is the mixing angle between ϕ and ω ($J = 1$, negative charge conjugation), a variety of measurements, expressed through the angle θ^- defined in Ref. (2), having given

$$\theta^-(J = 1) = -4^\circ \pm 1^\circ. \quad (\text{VI.9})$$

In Ref. (2) this mixing angle at fixed t rather than at fixed J is related to $k(t)$ by

$$\theta^-(t) \approx \frac{-\sqrt{2} \text{Re } k(t)}{\alpha_\omega(t) - \alpha_\phi(t)}, \quad (\text{VI.10})$$

so, if we interpret (VI.9) as referring to t at the mean of m_ω^2 and m_ϕ^2 , we have

$$\text{Re } k(t = 0.8 \text{ GeV}^2) \approx 0.02. \quad (\text{VI.11})$$

This value accords with (VI.8), confirming a marked drop from the value of k at $t = 0$ although we have no evidence for a continued fall as t increases beyond t_c . Both the sign and order of magnitude of $k(t)$ are as expected from our mechanism.

The major source of uncertainty in comparing with experiment arises from the non-negligible imaginary parts of the trajectories--as evidenced by the resonance widths. Within the moderate- t interval in question these imaginary parts are of the same order of magnitude as the real parts of the cylinder shift. Only if resonance widths decrease with increasing resonance mass can we look forward to a quantitatively clean comparison between theory and experiment.

C. Pseudoscalar Mesons

Any mechanism for the OZI rule and its breaking must account for the failure of pseudoscalar mesons to exhibit ideal nonet structure to the degree manifested by vector and tensor mesons. The π - η mass difference is much larger than that between ρ and ω and the η - η' mixing angle is displaced at least 40° from the ideal, in contrast to the 4° ω - ϕ displacement. The mechanism studied in this paper predicts cylinder quenching for unnatural-parity mesons but with a larger characteristic quenching interval than for natural parity--perhaps by as much as a factor 5--because of the small pion mass. We consequently expect, if $k_u(t)$ is defined to be the cylinder coupling between unnatural-parity planar poles, that throughout the mass range of the pseudoscalar nonet where $t < 1 \text{ GeV}^2$; we shall have $k_u(t)$ diminished little from $k_u(0)$. The π - η mass difference and the η - η' mixing angle correspond to $k_u \approx 0.3$, a number which is large compared to (VI.11) but of the same order as (VI.5). The anomalously-

00004400243

large non-planarity of the pseudoscalar nonet we thus attribute to the anomalously-small pseudoscalar mass. Particles of higher mass along unnatural-parity trajectories we expect to exhibit a degree of planarity higher than that shown by the leading pseudoscalars.

D. The New Particles

We come finally to the ψ particles, for which the OZI-rule has been widely invoked to explain the narrow widths, assuming the existence of a quantum number such as charm in addition to electric charge and strangeness. What does our mechanism have to say here?

If the perturbative rules of Ref. (2) are extended straightforwardly to the new quantum number, the coupling of a ψ trajectory to a trajectory of type n is (Eq. IV.5 of Ref. 2)

$$g_n^\psi(t) = \frac{\langle n | C(t) | \psi \rangle}{\alpha_\psi(t) - \alpha_n(t)}, \quad (\text{VI.12})$$

a mixing prescription identical to that proposed by other authors without invoking the topological expansion. The smallness of ψ mixing relative to that of ϕ is usually attributed to the large spacing between α_ψ and α_n , i.e. to a large denominator in (VI.12). The topological mechanism of the present paper, however, has been seen in Secs. III and V to yield two additional sources of relative smallness for ψ mixing: Because $C(t)$ falls with increasing t , the mixing matrix element itself decreases with increasing particle mass, and, if the lowest-lying mesons carrying the new quantum number are more massive than the ρ , the rate of cylinder suppression with increasing t will be greater along ψ trajectories than along ω and ϕ trajectories.

In principle any cylinder matrix element may be calculated from a knowledge of the planar S matrix, but we shall not here attempt a quantitative estimate of ψ -particle widths. A host of detailed questions, such as the sequence of ω and ϕ daughters, must be faced in order to achieve meaningful numbers.

VII. CONCLUSION

Veneziano motivated his topological expansion entirely by the smallness of $1/N^2$ (N characterizing the number of effective hadronic internal degrees of freedom)¹ without regard for the values of invariants such as t . This paper has identified a mechanism that tends to suppress cylinder components of the expansion in the physical- (positive- t) region, and since all higher components in the topological expansion involve "handles" closely related to cylinders, our mechanism may be presumed to affect the general convergence properties of the expansion. Asymptotic planarity becomes plausible at least along leading trajectories--not only the cylinder but all corrections to the planar S matrix becoming progressively smaller as t grows in a positive sense. The converse statement is also reasonable, merging with the familiar idea that, as t becomes negative, multi-pomeron cuts (multi-handles) grow in importance. A less familiar idea to which we have drawn attention is that the pomeron should become a purer singlet as t increases negatively.

A by-product of any mechanism for asymptotic planarity is an explanation of why leading trajectories are almost real (linear) at large positive t . Because imaginary parts of planar and twisted loops are equal, up to a sign, a mechanism that makes the planar loop larger

than the twisted loop must make the combined real part large compared to the combined imaginary part.

Asymptotically-free gauge theories, in contrast to the topological expansion, associate violation of the OZI rule (deviation from ideal mixing) with virtual gluon intermediate states. Gluon couplings are supposed to become progressively weaker with increasing t ,¹⁰ giving the same qualitative physical effect as our quenching of the cylinder. For large t both standpoints predict a gentle approach to the ideal mixing limit, but the observed rapid small- t development of ideal mixing along vector-tensor trajectories has been mysterious from the field-theoretical point of view. From our S-matrix standpoint, "precocious planarity" occurs whenever the lowest physical-particle masses important for the reggeon loop integrals are not much smaller than 1 GeV; the factor $2\pi^2$ in Formula (II.8) is an important ingredient.*

Should the pion mass be important in a reggeon loop integral, the development of planarity along coupled trajectories would be relatively slow. We conjecture that the large deviation from ideal mixing of the pseudoscalar mesons is due to their being coupled to loops where pions play a major role.

Finally, it may be observed that a monotonic variation of cylinder strength with t , whatever the underlying mechanism, leads to a clear operational meaning for the identity of pomeron and f : The leading Regge trajectory exhibits ideal mixing at large positive t and gradually shifts to a pure singlet character at large negative t .

* One may hope that an analogous factor will explain precocious scaling in the deep inelastic regime for lepton-hadron collisions.

ACKNOWLEDGMENTS

We have been greatly stimulated in this work by conversations with L. Balazs, J. Bronzan, J. Dash, H. Lipkin, C. Schmid, G. Veneziano, B. Webber, and A. White. While preparing our manuscript we received a preprint from M. Bishari¹¹ describing the same mechanism for cylinder quenching that has been discussed here.

0.0004408244

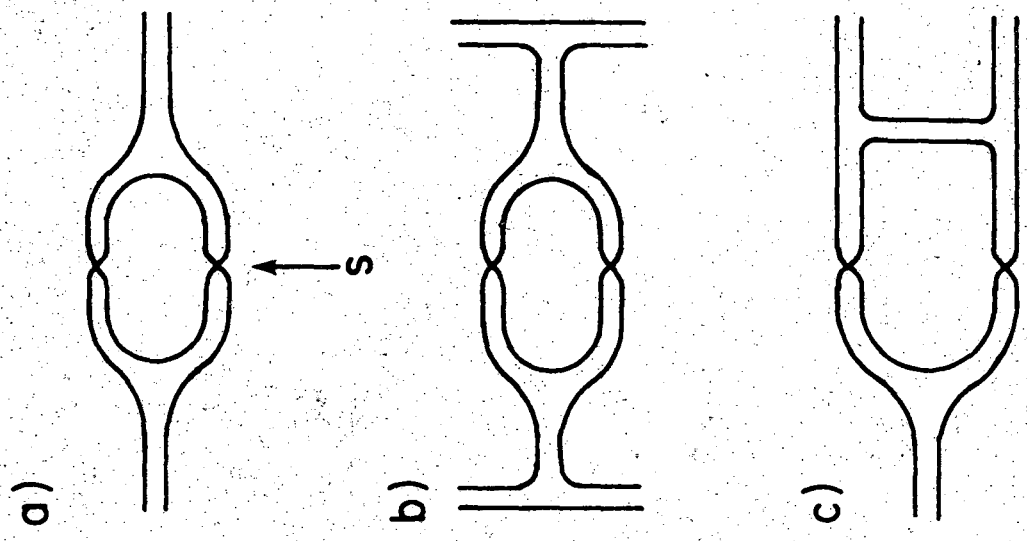
REFERENCES

- * This work was supported in part by the U. S. Energy and Research Development Administration (ERDA) and in part by an NSF contract, number MPS74-08175-A01.
1. G. Veneziano, Phys. Letters 52B, 220 (1974); Nucl. Phys. B74, 365 (1974).
 2. G. F. Chew and C. Rosenzweig, Lawrence Berkeley Laboratory report LBL-4201 (1975), to be published in the Physical Review; Phys. Letters 58B, 93 (1975).
 3. C. Schmid and C. Sorensen, Nucl. Phys. B96, 209 (1975);
C. Schmid, N. Papadapoulos, C. Sorensen, and D. Webber, ETH preprint (1975).
 4. N. Sakai, Rutherford Laboratory preprint RL75-094 (1975).
 5. M. Ciafaloni, C. DeTar, and M. Misheloff, Phys. Rev. 188, 2522 (1969).
 6. C. Rosenzweig and G. Veneziano, Phys. Letters 52B, 335 (1974).
 7. M. Schaap and G. Veneziano, Nuovo Cimento Letters 12, 204 (1975).
 8. M. Bishari and G. Veneziano, Weizmann Institute preprint (1975).
 9. Chan H. M., J. Paton and Tsou S. T., Nucl. Phys. B86, 479 (1974).
 10. J. Applegate and H. D. Politzer, Phys. Rev. Letters 34, 43 (1975).
 11. M. Bishari, Weizmann Institute preprint (1975).

FIGURE CAPTIONS

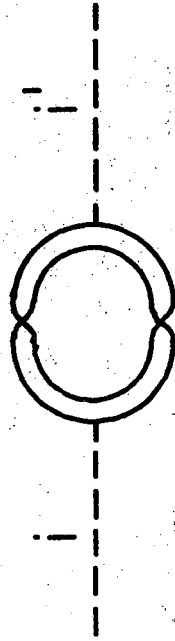
- Fig. 1a. A nonplanar duality diagram symbolizing the cylinder.
- 1b. The cylinder in its role as pomeron.
- 1c. The cylinder in its OZI-rule-violating role.
- Fig. 2. Diagrammatic representation of a cylinder-operator matrix element $\langle i|C(t)|i' \rangle$ connecting planar Regge poles.
- Fig. 3. Helicity-pole expansion of Fig. 2, the cross indicating twisted links.
- Fig. 4. Twisted loop with the same (vector-tensor) trajectory in both internal and external links.
- Fig. 5. Two-pion loop coupled to a leading trajectory of the vector-tensor family.
- Fig. 6. Loop with a pion link, coupled to a pseudoscalar trajectory.
- Fig. 7. Contour in w after first threshold in t has been passed.
- Fig. 8. Low- t and high- t estimates of cylinder quenching along leading vector-tensor trajectories.
- Fig. 9. The pattern of leading vector-tensor trajectories according to Ref. (2).

90004408245



XBL 7510-8588

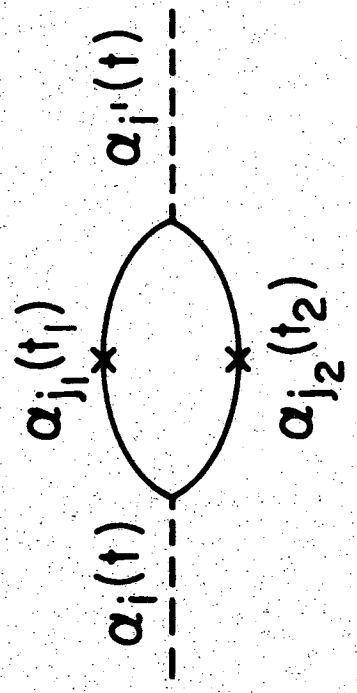
Fig. 1



XBL 7510-8589

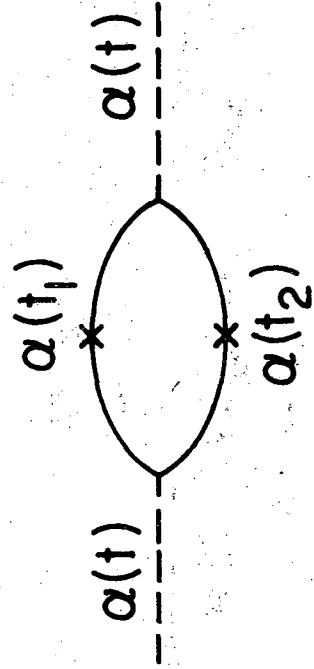
Fig. 2

00004408246



XBL 7510-8590

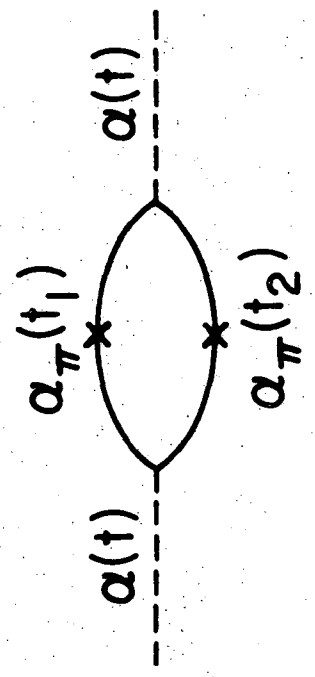
Fig. 3



XBL 7510-8591

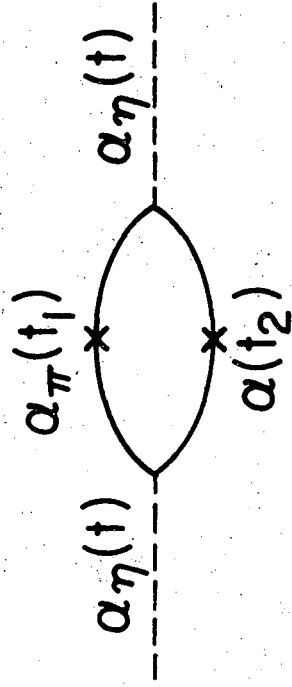
Fig. 4

00404406247



XBL 7510-8592

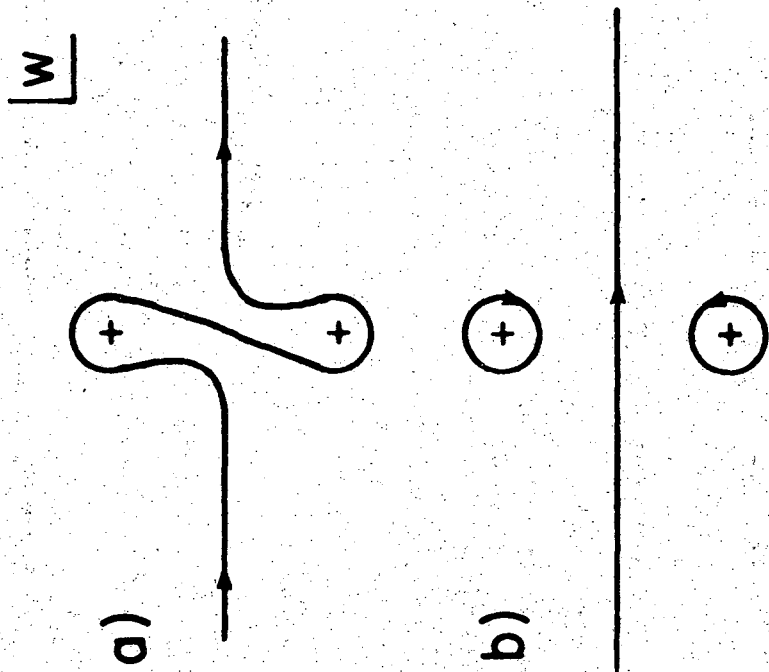
Fig. 5



XBL 7510-8593

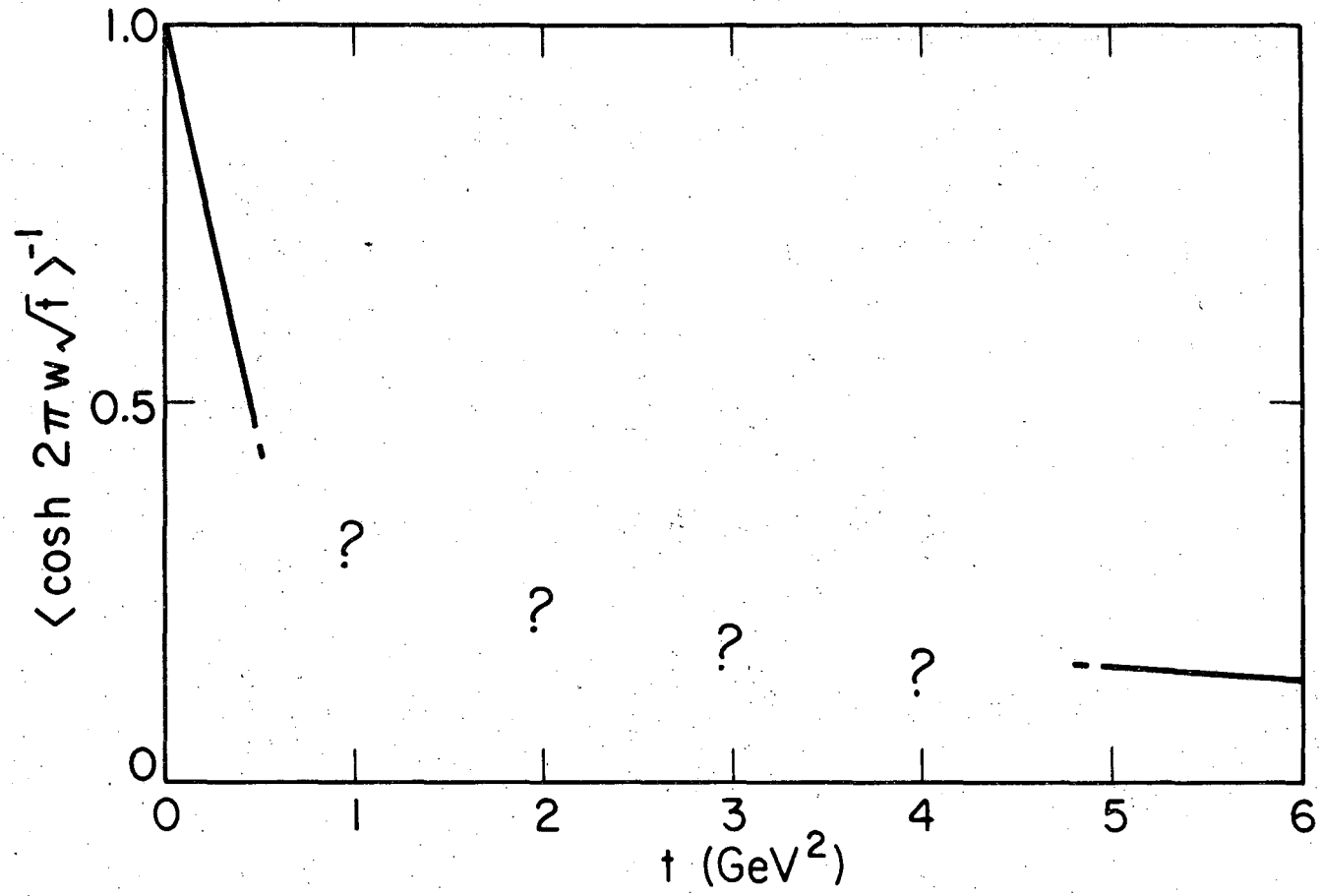
Fig. 6

90004408248



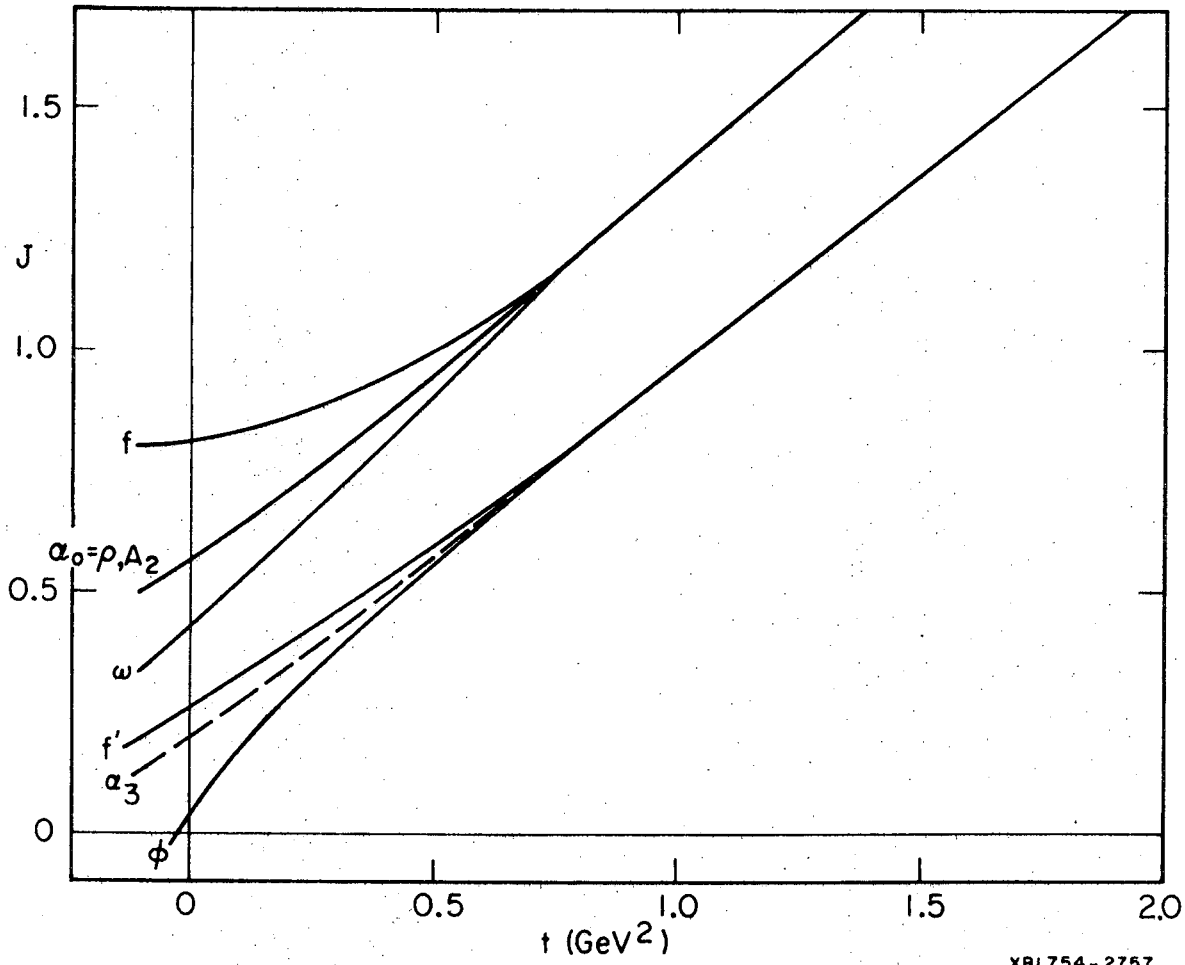
XBL 7510-8594

Fig. 7



XBL 7510-8595

Fig. 8



XBL754-2757

Fig. 9

LEGAL NOTICE

This report was prepared as an account of work sponsored by the United States Government. Neither the United States nor the United States Energy Research and Development Administration, nor any of their employees, nor any of their contractors, subcontractors, or their employees, makes any warranty, express or implied, or assumes any legal liability or responsibility for the accuracy, completeness or usefulness of any information, apparatus, product or process disclosed, or represents that its use would not infringe privately owned rights.

TECHNICAL INFORMATION DIVISION
LAWRENCE BERKELEY LABORATORY
UNIVERSITY OF CALIFORNIA
BERKELEY, CALIFORNIA 94720